Path-Independent Quantum Gates with Noisy Ancilla

Wen-Long Ma,[1,2,3] Mengzhen Zhang,[1,2,3] Yat Wong[ORCID],[1] Kyungjoo Noh,[1,2,3] Serge Rosenblum[ORCID],[2,3,4]
Philip Reinhold,[2,3] Robert J. Schoelkopf,[2,3] and Liang Jiang[ORCID][1,2,3]

[1]*Pritzker School of Molecular Engineering, University of Chicago, Illinois 60637, USA*
[2]*Department of Applied Physics and Physics, Yale University, New Haven, Connecticut 06511, USA*
[3]*Yale Quantum Institute, Yale University, New Haven, Connecticut 06511, USA*
[4]*Department of Condensed Matter Physics, Weizmann Institute of Science, Rehovot 76100, Israel*

Ancilla systems are often indispensable to universal control of a nearly isolated quantum system. However, ancilla systems are typically more vulnerable to environmental noise, which limits the performance of such ancilla-assisted quantum control. To address this challenge of ancilla-induced decoherence, we propose a general framework that integrates quantum control and quantum error correction, so that we can achieve robust quantum gates resilient to ancilla noise. We introduce the path independence criterion for fault-tolerant quantum gates against ancilla errors. As an example, a path-independent gate is provided for superconducting circuits with a hardware-efficient design.

An outstanding challenge of quantum computing is building quantum devices with both excellent coherence and reliable universal control [1–3]. For good coherence, we may choose physical systems with low dissipation (e.g., superconducting cavities [4–6] and nuclear spins [7–10]) or further boost the coherence with active quantum error correction [11,12]. As we improve the coherence by better isolating the central system from the noisy environment, it becomes more difficult to process information stored in the central system. To control the nearly isolated central system, we often introduce an ancilla system (e.g., transmon qubits [13–15] and electron spins [8,9]) that is relatively easy to control, but the ancilla system typically suffers more decoherence than the central system, limiting the fidelity of the ancilla-assisted quantum operations. Therefore, it is crucial to develop quantum control protocols that are fault-tolerant against ancilla errors.

For noise with temporal or spatial correlations, we can use techniques of dynamical decoupling [16–18] or decoherence-free encoding [19,20] to achieve noise-resilient control of the central system. When the noise has no correlations (e.g., Markovian noise), we need active quantum error correction (QEC) to extract the entropy. For qubit systems, a common strategy to suppress ancilla errors is to use the transversal approach [1,21–26], which may have a significant hardware overhead and cannot provide universal control [1], and it is desirable to have a hardware-efficient approach to fault-tolerant operations against ancilla errors [27–32]. Different from qubit systems, each bosonic mode has a large Hilbert space that can encode quantum information using various bosonic quantum codes as demonstrated in recent experiments [11,33–35]. However, there is no simple way to divide the bosonic

mode into separate subsystems, which prevents us from extending the transversal approach to the bosonic central system. Ancilla errors can propagate to the bosonic mode and compromise the encoded quantum information [36]. Nevertheless, a recent experiment with a hardware-efficient three-level ancilla demonstrated fault-tolerant readout of an error syndrome of the central system against the decay of the ancilla [37]. Moreover, the error-transparent gates for QEC codes (using control Hamiltonian commuting with errors) have been proposed [38–40] to achieve quantum operations insensitive to errors, but it is typically very demanding to fulfill the error-transparent condition while performing nontrivial quantum gates. Therefore, there is an urgent need of a general theoretical framework that integrates quantum control and quantum error correction, to guide the design of hardware-efficient robust quantum operations against ancilla errors.

In this Letter, we provide a general criterion for fault-tolerant quantum gates on the central system robust against ancilla errors [Fig. 1(a)]. Our general criterion of path independence (PI) requires that, for given initial and final ancilla states, the central system undergoes a unitary gate independent of the specific ancilla path induced by control drives and ancilla error events [Figs. 1(b) and 1(c)]. For a subset of final ancilla states, the desired quantum gate on the central system is successfully implemented, while other final ancilla states herald a failure of the attempted operation, but the central system still undergoes a deterministic unitary evolution without loss of coherence. Thus we may repeat our attempts of PI gates on the central system until the gate succeeds. As an application of our general criterion, a PI design of the selective number-dependent arbitrary phase (SNAP) gates [14,15] is provided
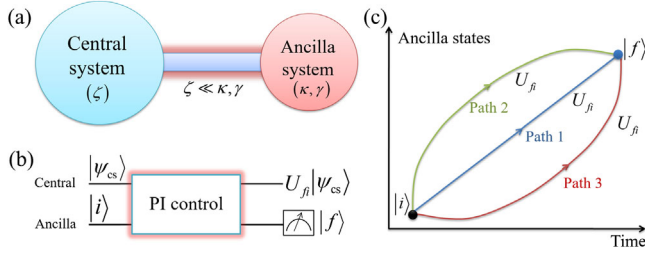
FIG. 1. (a) Schematic of a central system with good coherence coupled to an ancilla system with poor coherence. The ancilla dephasing rate κ and relaxation rate γ of are much larger than the decoherence rate ζ of the central system. (b),(c) For PI control, the central system undergoes a unitary evolution U_{fi} for the ancilla starting from state $|i\rangle$ and finally measured in $|f\rangle$, regardless of the ancilla paths induced by the control and ancilla error events.

for universal control and quantum error correction of superconducting circuits. Moreover, the error-transparent gates [38–40] are also shown to be a special class of PI gates.

Ancilla-assisted quantum control.—Suppose we intend to implement some unitary gate on the central system assisted by a d-level ancilla system. The total Hamiltonian is

$$H_{\mathrm{tot}}(t) = H_0 + H_c(t), \qquad (1)$$

where $H_c(t)$ is the control Hamiltonian and $H_0 = H_{\mathrm{as}} + H_{\mathrm{cs}} + H_{\mathrm{int}}$ is the static Hamiltonian with contributions from the ancilla system, the central system, and their interaction, correspondingly. We assume that $[H_{\mathrm{as}}, H_{\mathrm{int}}] = 0$, so that H_{int} preserves the eigenbasis $\{|m\rangle\}_{m=0}^{d-1}$ of the ancilla ($H_{\mathrm{as}}|m\rangle = \varepsilon_m|m\rangle$). The static Hamiltonian H_0 can be diagonalized in the eigenbasis of the ancilla,

$$H_0 = \sum_{m=0}^{d-1} |m\rangle\langle m| \otimes (\varepsilon_m + H_{\mathrm{cs}} + H_{\mathrm{int},m}), \qquad (2)$$

with $H_{\mathrm{int},m} = \langle m|H_{\mathrm{int}}|m\rangle$. The propagator for total system in the ancilla eigenbasis is

$$
\begin{aligned}
U(t_2, t_1) &= \mathcal{T} \exp\left(-i \int_{t_1}^{t_2} H_{\mathrm{tot}}(t')dt'\right) \\
&= \sum_{m,n} \eta_{mn}(t_2, t_1)|m\rangle\langle n| \otimes V_{mn}(t_2, t_1), \quad (3)
\end{aligned}
$$

where $\mathcal{T}$ is the time-ordering operator, $\eta_{mn}(t_2, t_1)$ is a complex function and $V_{mn}(t_2, t_1)$ is an operator on the central system. For preselection of the ancilla on state $|i\rangle$ at time t_1 and postselection on $|f\rangle$ at t_2, the central system undergoes a quantum operation $V_{mn}(t_2, t_1)$.

Markovian ancilla noise.—We assume that the central system suffers much weaker noise than the ancilla and therefore can be regarded as noise free within the ancilla

coherence time [Fig. 1(a)]. Suppose the ancilla suffers from Markovian noise and the dynamics of the total system is

$$\frac{d\rho}{dt} = i[\rho, H_{\mathrm{tot}}(t)] + \left(\sum_l \mathcal{D}[\sqrt{\kappa_l}L_l] + \sum_j \mathcal{D}[\sqrt{\gamma_j}J_j]\right)\rho, \qquad (4)$$

where $D[A]\rho = A\rho A^\dagger - \{A^\dagger A, \rho\}/2$ is the Lindbladian dissipator, $\{L_l\}/\{J_j\}$ are the Lindblad operators describing the ancilla dephasing and relaxation errors ($L_l = \sum_{m=0}^{d-1} \Delta_l^{(m)}|m\rangle\langle m|$ with $\Delta_l^{(m)} \in \mathbb{C}$, $J_j = |m_j\rangle\langle n_j|$ with $m_j, n_j \in [0, d-1]$ and $m_j \neq n_j$), and κ_l/γ_j is the dephasing and relaxation rate. The ancilla dephasing and relaxation errors can be unified into a general class of ancilla errors [41].

The Liouville superoperator $\mathcal{L}(t)$ generating the Markovian dynamics in Eq. (4) can be divided into two parts [43],

$$\frac{d\rho}{dt} = \mathcal{L}(t)\rho(t) = [\mathcal{L}_{\mathrm{eff}}(t) + \mathcal{S}]\rho(t), \qquad (5)$$

where $\mathcal{L}_{\mathrm{eff}}\rho = i(\rho H_{\mathrm{eff}}^\dagger - H_{\mathrm{eff}}\rho)$ represents the no-jump evolution with $H_{\mathrm{eff}}(t) = H_{\mathrm{tot}}(t) - \frac{i}{2}(\sum_l \kappa_l L_l^\dagger L_l + \sum_j \gamma_j J_j^\dagger J_j)$, and $\mathcal{S}\rho = \sum_l \kappa_l L_l \rho L_l^\dagger + \sum_j \gamma_j J_j \rho J_j^\dagger$ represents the quantum jumps interrupting the no-jump evolution. The propagator for the whole system can be represented by the generalized Dyson expansion as

$$\rho(t) = \sum_{p=0}^{\infty} \mathcal{G}_p(t, 0)\rho(0), \qquad (6)$$

with

$$\mathcal{G}_0(t, 0) = \mathcal{W}(t, 0), \qquad (7)$$

$$
\begin{aligned}
\mathcal{G}_p(t, 0) &= \int_0^t dt_p \cdots \int_0^{t_3} dt_2 \int_0^{t_2} dt_1 \mathcal{W}(t, t_p) \\
&\times \mathcal{S} \cdots \mathcal{S}\mathcal{W}(t_2, t_1)\mathcal{S}\mathcal{W}(t_1, 0), \quad p \geq 1, \quad (8)
\end{aligned}
$$

where $\rho(0) = |m\rangle\langle m| \otimes \rho_{\mathrm{cs}}$ with $m \in [0, d-1]$ and ρ_{cs} being the initial density matrix of the central system, and $\mathcal{W}(t_2, t_1)\rho = W(t_2, t_1)\rho W^\dagger(t_2, t_1)$ with $W(t_2, t_1) = \mathcal{T} \exp[-i \int_{t_1}^{t_2} H_{\mathrm{eff}}(t')dt']$ being the no-jump propagator. $\mathcal{G}_p(t, 0)$ contains all the paths with any sequence of p ancilla jump events, therefore describing the pth-order ancilla errors. When $\kappa_l t, \gamma_j t \ll 1$, the Liouville superoperator is well approximated by a finite-order Dyson expansion.

Definition of path independence.—The PI gates in this Letter can be understood as follows. With an initial ancilla eigenstate $|i\rangle$ of H_{as}, some control Hamiltonian acting

during $[0, t]$ and a final projective measurement on the ancilla with result $|r\rangle$, the central system undergoes a deterministic unitary evolution up to finite-order or infinite-order Dyson expansion in Eq. (6). Now we provide a formal definition of path independence.

Definition 1: path independence. Let the ancilla start from $|i\rangle$ and end in $|r\rangle$, with $|i\rangle, |r\rangle \in \{|m\rangle\}_{m=0}^{d-1}$. Suppose that

$$\langle r| \left[\sum_{p=0}^{k} \mathcal{G}_p(t,0)(|i\rangle\langle i| \otimes \rho_{cs}) \right] |r\rangle \propto \mathcal{U}_{ri}(t,0)\rho_{cs} \quad (9)$$

applies for $k \le n$ but does not hold for $k > n$, where $\mathcal{U}_{ri}(t,0)\rho_{cs} = U_{ri}(t,0)\rho_{cs}U_{ri}^\dagger(t,0)$ is a unitary channel on the central system. Then we say the central system gate is PI of the ancilla errors up to the nth order from $|i\rangle$ to $|r\rangle$.

Path independence for ancilla dephasing errors.—The path independence for ancilla dephasing errors is guaranteed if the no-jump propagator is in a PI form below.

Lemma 1. Let $\{U_{mn}(t_2, t_1)\}_{m,n=0}^{d-1}$ be a set of unitaries on the central system that are differentiable with respect to t_2 and t_1 and also satisfy the PI condition

$$U_{me}(t_3, t_2)U_{en}(t_2, t_1) = U_{mn}(t_3, t_1), \quad (10)$$

with $m, e, n \in [0, d-1]$ and $t_1, t_2, t_3 \in \mathbb{R}$, there exist a class of PI no-jump propagators

$$W(t_2, t_1) = \sum_{m,n} \xi_{mn}(t_2, t_1)|m\rangle\langle n| \otimes U_{mn}(t_2, t_1), \quad (11)$$

where $\{\xi_{mn}(t_2, t_1)\}_{m,n=0}^{d-1}$ are a set of complex functions of t_2 and t_1 satisfying $\xi_{mn}(t_3, t_1) = \sum_{e=0}^{d-1} \xi_{me}(t_3, t_2)\xi_{en}(t_2, t_1)$ and $\xi_{mn}(t, t) = \delta_{mn}$.

Note that here we define all the unitaries in the set $\{U_{mn}(t_2, t_1)\}_{m,n=0}^{d-1}$, but typically only a subset of $\{U_{mn}(t_2, t_1)\}_{m,n=0}^{d-1}$ with $\xi_{mn}(t_2, t_1) \ne 0$ contribute to the no-jump dynamics and the other unitaries in the set with $\xi_{mn}(t_2, t_1) = 0$ can be left undefined.

Lemma 2. The PI condition for $\{U_{mn}(t_2, t_1)\}_{m,n=0}^{d-1}$ in Eq. (10) is satisfied if and only if

$$U_{mn}(t_2, t_1) = R_m(t_2)U_{mn}R_n^\dagger(t_1), \quad (12)$$

where $R_m(t) = \mathcal{T}\{e^{-i\int_0^t H_m(t')dt'}\}$ with $H_m(t)$ being an arbitrary time-dependent Hamiltonian on the central system and $\{U_{mn}\}_{m,n=0}^{d-1} = \{U_{mn}(0,0)\}_{m,n=0}^{d-1}$ satisfy

$$U_{me}U_{en} = U_{mn}. \quad (13)$$

Theorem 1: dephasing errors. With the PI no-jump propagator in Eq. (11) and only ancilla dephasing errors, the central system gate is PI of all ancilla dephasing
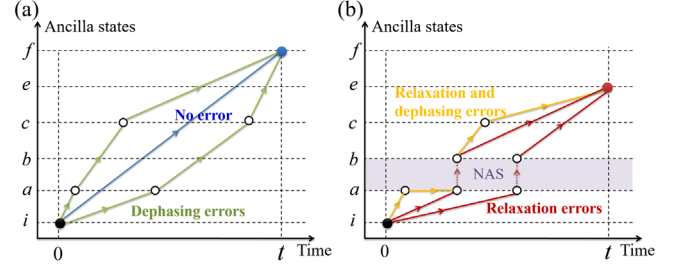

FIG. 2. Schematic of ancilla evolution paths with different kinds of ancilla errors. (a) In the paths with blue line, the ancilla goes from $|i\rangle$ to $|f\rangle$ without any ancilla error and the central system gate is U_{fi}. In the paths with green lines, the ancilla suffers two dephasing errors $|a\rangle\langle a|$ and at $|c\rangle\langle c|$, while the central system gate is still $U_{fc}U_{ca}U_{ai} = U_{fi}$, independent of the dephasing error times. (b) In the paths with red lines, the ancilla suffers a relaxation error $|b\rangle\langle a|$ (dashed red arrow lines) in the NAS spanned by $\{|a\rangle, |b\rangle\}$ (purple-shaded region) with the unitary gate as $U_{eb}U_{ai}$. In the paths with yellow line, the ancilla suffers two additional dephasing errors $|a\rangle\langle a|$ and $|c\rangle\langle c|$ but with the same unitary gate as that for a single relaxation error. The solid (hollow) circles represent the initial and final (intermediate) ancilla states, and the red dashed arrows represent the ancilla relaxation errors. Here we adopt the interaction picture associated with $H_0'(t)$.

errors up to infinite order from $|i\rangle$ to $|r\rangle$ for all $|i\rangle, |r\rangle \in \{|m\rangle\}_{m=0}^{d-1}$.

To understand Theorem 1, we move to the interaction picture associated with $H_0'(t) = \sum_{m=0}^{d-1} |m\rangle\langle m| \otimes H_m(t)$ [note that H_0 in Eq. (2) and $H_0'(t)$ are similar but can be different]. The no-jump propagator becomes

$$W^{(I)}(t_2, t_1) = \sum_{m,n} \xi_{mn}(t_2, t_1)|m\rangle\langle n| \otimes U_{mn}, \quad (14)$$

and the ancilla dephasing operator $L_l^{(I)}(t_1) = L_l$ acts trivially on the central system regardless of the jump time t_1. Suppose the ancilla suffers a dephasing error $L^{(I)}(t_1)$ at time $t_1 \in [0, t]$, the quantum operation on the central system is

$$\langle r|W^{(I)}(t, t_1)L^{(I)}(t_1)W^{(I)}(t_1, 0)|i\rangle \propto U_{ri}, \quad (15)$$

where we have used Eq. (13). So independent of the error time t_1, the central system undergoes the same unitary gate as that without any ancilla error $[\langle r|W^{(I)}(t, 0)|i\rangle \propto U_{ri}]$. The conclusion holds for arbitrary number of dephasing jumps during the gate, since $U_{ri} = U_{re} \cdots U_{ba}U_{ai}$ with $a, b, \ldots, e \in [0, d-1]$ from Eq. (13). An intuitive picture is provided in Fig. 2(a). Without ancilla errors [blue path in Fig. 2(a)], the ancilla goes directly from the initial state to the final state with the target central system gate. With ancilla dephasing errors [green paths in Fig. 2(a)], the ancilla takes different continuous paths between the same

initial and final states, but the central system gate remains unchanged since it depends only on the initial and final ancilla states.

Path independence for ancilla relaxation errors.—The path independence for ancilla relaxation errors is slightly more demanding than that for ancilla dephasing errors. To see this, suppose the ancilla suffers a relaxation error $J^{(I)}(t_1) = |m\rangle\langle n| \otimes R_m^\dagger(t_1)R_n(t_1)$ at time t_1, the final quantum operation on the central system is

$$\langle r|W^{(I)}(t,t_1)J^{(I)}(t_1)W^{(I)}(t_1,0)|i\rangle$$
$$\propto U_{rm}R_m^\dagger(t_1)R_n(t_1)U_{ni}, \qquad (16)$$

which is typically a unitary gate depending on t_1, causing decoherence of the central system when averaged over t_1. This can be avoided if $R_m^\dagger(t_1)R_n(t_1) \propto e^{i\Delta\lambda t_1}$ or $H_m(t) - H_n(t) = \Delta\lambda$ with $\Delta\lambda \in \mathbb{R}$. So the following definition is motivated.

Definition 2: noiseless ancilla subspace. We denote the ancilla subspace spanned by $\{|k\rangle\} \subset \{|m\rangle\}_{m=0}^{d-1}$ satisfying $H_m(t) + \lambda_m(t) = H_n(t) + \lambda_n(t)$ with $\lambda_m(t), \lambda_n(t) \in \mathbb{R}$ for all $|m\rangle, |n\rangle \in \{|k\rangle\}$ as the noiseless ancilla subspace (NAS).

Path independence of first-order ancilla relaxation errors is guaranteed if the same unitary operation is applied to the central system for all possible paths from $|i\rangle$ to $|r\rangle$ with at most one ancilla relaxation jump. For example, if $\xi_{ri} \neq 0$ and there are no paths with first-order relaxation errors from $|i\rangle$ to $|r\rangle$, the central system gate is still U_{ri}, or if $\xi_{ri} = 0$ and the only path from $|i\rangle$ to $|r\rangle$ is through a relaxation operator $J^{(I)}$ in the NAS, then the central system gate is $U_{rm}U_{ni}$ [this is equivalent to redefining $U_{ri} = U_{rm}U_{mn}U_{ni}$ by setting $U_{mn} = \mathbb{I}$ as the identity operation, since U_{ri} in Eq. (14) is not well defined if $\xi_{ri} = 0$]. The conclusion can be extended to the cases for higher-order relaxation errors.

Theorem 2: relaxation and dephasing errors. With the PI no-jump propagator in Eq. (11) and both ancilla relaxation and dephasing errors, if all the possible paths from $|i\rangle$ to $|r\rangle$ with at most n sequential ancilla relaxation jumps, only include either the path without relaxation errors or the paths consisting of no more than n sequential ancilla relaxation jumps in the NAS, and these paths produce the same unitary gate on the central system, which does not hold for all the paths from $|i\rangle$ to $|r\rangle$ with at most $(n + 1)$ sequential ancilla relaxation jumps, then the central system gate is PI of the combination of up to the nth-order ancilla relaxation errors and up to infinite-order ancilla dephasing errors from $|i\rangle$ to $|r\rangle$.

Theorem 2 can be intuitively understood by the diagrams in Fig. 2(b). With only ancilla relaxation errors in the NAS [red paths in Fig. 2(b)], the ancilla path is composed of discontinuous segments connected by the relaxation error operators, and the final unitary gate on the central system is

often different from that without ancilla errors. However, if the ancilla ends in another state, the central system still undergoes a deterministic unitary evolution. With both ancilla relaxation errors in the NAS and dephasing errors [orange paths in Fig. 2(b)], for each path segment connected by the relaxation errors, the ancilla goes another continuous way with the same initial and final states, so the final unitary gate on the central system is the same as that with only relaxation errors.

A special case of PI gates is the error-transparent gates, theoretically proposed [38,39] and recently experimentally demonstrated [40] against a specific system error, with the error syndromes corresponding to the ancilla states here. Error transparency requires the physical Hamiltonian to commute with the errors when acting on the QEC code subspace (a more general condition for error transparency is that the commutator of the physical Hamiltonian and the error operator is proportional to the error operator), corresponding to a PI no-jump propagator [Eq. (11)] with $\xi_{mn} = 0$ for $m \neq n$ and all the ancilla errors are relaxation errors $|m\rangle\langle n|$ in the NAS, and thus fulfill the PI criterion. However, the PI gates contain a larger set of operations, because the PI criterion can be fulfilled with non-error-transparent Hamiltonians (see the Supplemental Material [41] for general construction of the PI control Hamiltonian and jump operators).

Example: PI gates in superconducting circuits.—We consider the implementation of the SNAP gates in superconducting circuits [14,15]. The superconducting cavity (central system) dispersively couples to a nonlinear transmon device (ancilla system) with Hamiltonian $H_0 = \omega_{ge}|e\rangle\langle e| + \omega_c a^\dagger a - \chi a^\dagger a|e\rangle\langle e|$ [5], where ω_{ge} (ω_c) is the transmon (cavity) frequency, a ($a^\dagger$) is the annihilation (creation) operator of the cavity mode, χ is the dispersive coupling strength, and $|e\rangle$ ($|g\rangle$) denotes the excited (ground) state of the ancilla transmon. The SNAP gate on the cavity, $S(\vec{\varphi}) = \sum_{n=0}^\infty e^{i\varphi_n}|n\rangle\langle n|$, imparts arbitrary phases $\vec{\varphi} = \{\varphi_n\}_{n=0}^\infty$ to the different Fock states of the cavity.

In the interaction picture associated with $H_0' = H_0 - \delta|e\rangle\langle e|$, the total Hamiltonian is $H_{\text{tot}}^{(I)} = \Omega[|g\rangle\langle e| \otimes S(\vec{\varphi}) + |e\rangle\langle g| \otimes S(-\vec{\varphi})] + \delta|e\rangle\langle e| = \Omega\sum_{n=0}^\infty(e^{i\varphi_n}|g,n\rangle\langle e,n| + e^{-i\varphi_n}|e,n\rangle\langle g,n|) + \delta|e\rangle\langle e|$, inducing a PI propagator [Eq. (14)] [41]. The original SNAP gate consists of two consecutive π pulses (between $|g,n\rangle$ and $|e,n\rangle$) with a geometric phase depending on the phase difference between the two π pulses. For simplicity, we may fix the phase of the second pulse to be 0, so that the geometric phase for the SNAP gate is determined by the phase φ_n of the first π pulse. Returning to the Schrödinger picture, $H_c(t) = \Omega\sum_{n=0}^\infty(e^{i[(\omega_{ge}-n\chi)t+\varphi_n-\delta]}|g,n\rangle\langle e,n| + \text{H.c.})$. When $\Omega \ll \chi$, the control Hamiltonian can be simplified as the driving acting on the transmon alone but with multiple frequency components, $H_c(t) \approx \epsilon_{ge}(t)e^{i(\omega_{ge}-\delta)t}|g\rangle\langle e| + \text{H.c.}$

with $\epsilon_{ge}(t) = \sum_n \Omega e^{i(\varphi_n - n\chi t)}$. Then the SNAP gates are PI of any transmon dephasing error with $\mathcal{D}[\sqrt{\gamma_1}(c_e|e\rangle\langle e| + c_g|g\rangle\langle g|)]$ with $c_{g/e} \in \mathbb{C}$ (see Theorem 1), but not PI of the transmon relaxation error with $\mathcal{D}[\sqrt{\kappa_1}(|g\rangle\langle e|)]$, since $\{|g\rangle, |e\rangle\}$ do not span a NAS (Theorem 2) [41].

To make the SNAP gates PI of the dominant transmon relaxation error, we use a three-level transmon with $H_0 = \omega_{ge}|e\rangle\langle e| + \omega_{gf}|f\rangle\langle f| + \omega_c a^\dagger a - \chi(|e\rangle\langle e| + |f\rangle\langle f|)a^\dagger a$, where the dispersive coupling strength is engineered to the same for the first-excited transmon state $|e\rangle$ and the second-excited state $|f\rangle$ [37]. The SNAP gate is implemented by applying the Hamiltonian that drives the $|g\rangle \leftrightarrow |f\rangle$ transition instead of the $|g\rangle \leftrightarrow |e\rangle$ transition (if the direct transition between $|g\rangle$ and $|f\rangle$ is not allowed, we can use Raman drives detuned from the $|g\rangle \leftrightarrow |e\rangle$ and $|e\rangle \leftrightarrow |f\rangle$ transitions). Since $\{|e\rangle, |f\rangle\}$ span a NAS, the SNAP gate is PI of the dominant transmon relaxation error with $\mathcal{D}[\sqrt{\kappa_2}(|e\rangle\langle f|)]$ and also of any transmon dephasing error with $\mathcal{D}[\sqrt{\gamma_2}(c_g|g\rangle\langle g| + c_e|e\rangle\langle e| + c_f|f\rangle\langle f|)]$. Note that the PI SNAP gates are not error transparent, but they still enable robustness against transmon errors.

PI gates for both ancilla errors and central system errors.—The PI gates for ancilla errors can also be made PI of the central system errors. We assume that the central system also suffers Markovian noise with the Lindbladian dissipators $\sum_{i=0}^{q-1} \mathcal{D}[\sqrt{\zeta_i}E_i]$. Suppose a quantum error correction (QEC) code exists for the central system [1,44,45], which means that the error set $\{E_i\}$ satisfies the Knill-Laflamme condition $P_0 E_i^\dagger E_j P_0 = A_{ij} P_0$ with $E_0 = P_0$ being the projection to the code subspace and A a Hermitian matrix. We may diagonalize A as $B = u^\dagger A u$ to obtain another set of correctable errors $\{F_k\}$ with $F_k = \sum_{ik} u_{ik} E_i$, satisfying $P_0 F_k^\dagger F_l P_0 = r_k \delta_{kl} P_0$ with $F_0 = P_0$, $B_{00} = 1$ and $r_k = B_{kk}$. Then the condition for path independence against the central system errors is

$$[H_0'(t), F_k] = \sum_{m=0}^{d-1} c_{m,k}(t)|m\rangle\langle m| \otimes F_k, \qquad (17)$$

where $m \in [0, d-1]$, $k \in [0, q-1]$ and $c_{m,k}(t) \in \mathbb{R}$. In the interaction picture associated with $H_0'(t)$, this condition ensures that $R^\dagger(t)F_k R(t) = \sum_m e^{i\int_{t_1}^{t_2} c_{m,k}(t')dt'}|m\rangle\langle m| \otimes F_k$ is a tensor product of the ancilla dephasing operator and the same error operator F_k with $R(t) = \mathcal{T}e^{-i\int_0^t H_0'(t')dt'}$. Then the PI no-jump propagator for both ancilla and central system errors [38,39,41] can be constructed as in Eq. (14) with

$$U_{mn} = \sum_k e^{i\phi_{mn,k}} F_k U_{mn,0} F_k^\dagger / r_k, \qquad (18)$$

where $U_{mn,0}$ is the target unitary in the code subspace satisfying $U_{mn,0} U_{mn,0}^\dagger = P_0$ and $\phi_{mn,k} \in \mathbb{R}$. After such a PI gate, we can make a joint measurement on both the ancilla

state and the error syndromes of the central system. The path independence of ancilla errors is then ensured and the first-order central system errors during the gate can also be corrected [41].

Summary.—To address the challenge of ancilla-induced decoherence, we provide a general criterion of path independence. For quantum information processing with bosonic encoding, such a PI design will be crucial in protecting the encoded information from ancilla errors, while the previous transversal approach does not apply. Moreover, different from the traditional approaches with separated quantum control and error correction tasks, our approach integrates quantum control and error correction. Using the general PI design, we can further explore PI gates using various kinds of ancilla systems to achieve higher-order suppression of ancilla errors, design PI operations robust against both ancilla errors and central system errors, and extend the PI technique to quantum sensing and other quantum information processing tasks.

Note added.—Recently the PI SNAP gates have been experimentally implemented in a superconducting circuits [42], with the SNAP gate fidelity significantly improved by the PI design.

[1] M. A. Nielsen and I. L. Chuang, *Quantum Computation and Quantum Information* (Cambridge University Press, New York, 2010).

[2] S. J. Glaser, U. Boscain, T. Calarco, C. P. Koch, W. Kockenberger, R. Kosloff, I. Kuprov, B. Luy, S. Schirmer, T. Schulte-Herbrggen, D. Sugny, and F. K. Wilhelm, Training Schrodinger's cat: Quantum optimal control: Strategic report on current status, visions and goals for research in Europe, Eur. Phys. J. D **69**, 279 (2015).

[3] L. Vandersypen and I. Chuang, NMR techniques for quantum control and computation, Rev. Mod. Phys. **76**, 1037 (2005).

[4] M. H. Devoret and R. J. Schoelkopf, Superconducting circuits for quantum information: An outlook, Science **339**, 1169 (2013).

[5] D. I. Schuster, A. A. Houck, J. A. Schreier, A. Wallraff, J. M. Gambetta, A. Blais, L. Frunzio, J. Majer, B. Johnson, M. H. Devoret, S. M. Girvin, and R. J. Schoelkopf,

Resolving photon number states in a superconducting circuit, Nature (London) **445**, 515 (2007).

[6] Z. Leghtas, G. Kirchmair, B. Vlastakis, R. J. Schoelkopf, M. H. Devoret, and M. Mirrahimi, Hardware-Efficient Autonomous Quantum Memory Protection, Phys. Rev. Lett. **111**, 120501 (2013).

[7] B. E. Kane, A silicon-based nuclear spin quantum computer, Nature (London) **393**, 133 (1998).

[8] M. V. G. Dutt, L. Childress, L. Jiang, E. Togan, J. Maze, F. Jelezko, A. S. Zibrov, P. R. Hemmer, and M. D. Lukin, Quantum register based on individual electronic and nuclear spin qubits in diamond, Science **316**, 1312 (2007).

[9] P. C. Maurer, G. Kucsko, C. Latta, L. Jiang, N. Y. Yao, S. D. Bennett, F. Pastawski, D. Hunger, N. Chisholm, M. Markham, D. J. Twitchen, J. I. Cirac, and M. D. Lukin, Room-temperature quantum bit memory exceeding one second, Science **336**, 1283 (2012).

[10] G.-Q. Liu, J. Xing, W.-L. Ma, P. Wang, C.-H. Li, H. C. Po, R.-B. Liu, and X.-Y. Pan, Single-Shot Readout of a Nuclear Spin Weakly Coupled to a Nitrogen-Vacancy Center, Phys. Rev. Lett. **118**, 150504 (2017).

[11] N. Ofek, A. Petrenko, R. Heeres, P. Reinhold, Z. Leghtas, B. Vlastakis, Y. Liu, L. Frunzio, S. M. Girvin, L. Jiang, M. Mirrahimi, M. H. Devoret, and R. J. Schoelkopf, Extending the lifetime of a quantum bit with error correction in superconducting circuits, Nature (London) **536**, 441 (2016).

[12] G. Waldherr, Y. Wang, S. Zaiser, M. Jamali, T. Schulte-Herbrggen, H. Abe, T. Ohshima, J. Isoya, J. F. Du, P. Neumann, and J. Wrachtrup, Quantum error correction in a solid-state hybrid spin register, Nature (London) **506**, 204 (2014).

[13] J. Koch, T. M. Yu, J. Gambetta, A. A. Houck, D. I. Schuster, J. Majer, A. Blais, M. H. Devoret, S. M. Girvin, and R. J. Schoelkopf, Charge-insensitive qubit design derived from the Cooper pair box, Phys. Rev. A **76**, 042319 (2007).

[14] S. Krastanov, V. V Albert, C. Shen, C. L. Zou, R. W. Heeres, B. Vlastakis, R. J. Schoelkopf, and L. Jiang, Universal control of an oscillator with dispersive coupling to a qubit, Phys. Rev. A **92**, 040303(R) (2015).

[15] R. W. Heeres, B. Vlastakis, E. Holland, S. Krastanov, V. V. Albert, L. Frunzio, L. Jiang, and R. J. Schoelkopf, Cavity State Manipulation Using Photon-Number Selective Phase Gates, Phys. Rev. Lett. **115**, 137002 (2015).

[16] L. Viola, E. Knill, and S. Lloyd, Dynamical Decoupling of Open Quantum Systems, Phys. Rev. Lett. **82**, 2417 (1999).

[17] T. H. Taminiau, J. Cramer, T. van der Sar, V. V Dobrovitski, and R. Hanson, Universal control and error correction in multi-qubit spin registers in diamond, Nat. Nanotechnol. **9**, 171 (2014).

[18] G.-Q. Liu, H. C. Po, J. Du, R.-B. Liu, and X.-Y. Pan, Noise-resilient quantum evolution steered by dynamical decoupling, Nat. Commun. **4**, 2254 (2013).

[19] D. A. Lidar, I. L. Chuang, and K. Whaley, Decoherence-Free Subspaces for Quantum Computation, Phys. Rev. Lett. **81**, 2594 (1998).

[20] D. Bacon, D. A. Lidar, and K. B. Whaley, Robustness of decoherence-free subspaces for quantum computation, Phys. Rev. A **60**, 1944 (1999).

[21] D. Gottesman, An introduction to quantum error correction and fault-tolerant quantum computation, in *Quantum Information Science and Its Contributions to Mathematics*, Proceedings of Symposia in Applied Mathematics Vol. 68 (American Mathematical Society, Providence, Rhode Island, 2010), pp. 13–58.

[22] E. Knill, R. Laflamme, and W. H. Zurek, Resilient quantum computation: Error models and thresholds, Proc. R. Soc. A **454**, 365 (1998).

[23] D. P. DiVincenzo and P. W. Shor, Fault-Tolerant Error Correction with Efficient Quantum Codes, Phys. Rev. Lett. **77**, 3260 (1996).

[24] B. Eastin and E. Knill, Restrictions on Transversal Encoded Quantum Gate Sets, Phys. Rev. Lett. **102**, 110502 (2009).

[25] A. G. Fowler, M. Mariantoni, J. M. Martinis, and A. N. Cleland, Surface codes: Towards practical large-scale quantum computation, Phys. Rev. A **86**, 032324 (2012).

[26] D. Gottesman, Quantum fault tolerance in small experiments, arXiv:1610.03507.

[27] R. Chao and B. W. Reichardt, Quantum Error Correction with Only Two Extra Qubits, Phys. Rev. Lett. **121**, 050502 (2018).

[28] R. Chao and B. W. Reichardt, Fault-tolerant quantum computation with few qubits, npj Quantum Inf. **4**, 42 (2018).

[29] C. Chamberland and M. E. Beverland, Flag fault-tolerant error correction with arbitrary distance codes, Quantum **2**, 53 (2018).

[30] C. Chamberland and A. W. Cross, Fault-tolerant magic state preparation with flag qubits, Quantum **3**, 143 (2019).

[31] C. Chamberland, G. Zhu, T. J. Yoder, J. B. Hertzberg, and A. W. Cross, Topological and Subsystem Codes on Low-Degree Graphs with Flag Qubits, Phys. Rev. X **10**, 011022 (2020).

[32] C. Chamberland, A. Kubica, T. J. Yoder, and G. Zhu, Triangular color codes on trivalent graphs with flag qubits, New J. Phys. **22**, 023019 (2020).

[33] C. Flühmann, T. L. Nguyen, M. Marinelli, V. Negnevitsky, K. Mehta, and J. P. Home, Encoding a qubit in a trapped-ion mechanical oscillator, Nature (London) **566**, 513 (2019).

[34] L. Hu, Y. Ma, W. Cai, X. Mu, Y. Xu, W. Wang, Y. Wu, H. Wang, Y. P. Song, C.-L. Zou, S. M. Girvin, L-M. Duan, and L. Sun, Quantum error correction and universal gate set operation on a binomial bosonic logical qubit, Nat. Phys. **15**, 503 (2019).

[35] P. Campagne-Ibarcq, A. Eickbusch, S. Touzard, E. Zalys-Geller, N. E. Frattini, V. V. Sivak, P. Reinhold, S. Puri, S. Shankar, R. J. Schoelkopf, L. Frunzio, M. Mirrahimi, and M. H. Devoret, Quantum error correction of a qubit encoded in grid states of an oscillator, Nature (London) **584**, 368 (2020).

[36] R. W. Heeres, P. Reinhold, N. Ofek, L. Frunzio, L. Jiang, M. H. Devoret, and R. J. Schoelkopf, Implementing a universal gate set on a logical qubit encoded in an oscillator, Nat. Commun. **8**, 94 (2017).

[37] S. Rosenblum, P. Reinhold, M. Mirrahimi, L. Jiang, L. Frunzio, and R. J. Schoelkopf, Fault-tolerant detection of a quantum error, Science **361**, 266 (2018).

[38] O. Vy, X. Wang, and K. Jacobs, Error-transparent evolution: The ability of multi-body interactions to bypass decoherence, New J. Phys. **15**, 053002 (2013).

[39] E. Kapit, Error-Transparent Quantum Gates for Small Logical Qubit Architectures, Phys. Rev. Lett. **120**, 050503 (2018).

[40] Y. Ma, Y. Xu, X. Mu, W. Cai, L. Hu, W. Wang, X. Pan, H. Wang, Y. P. Song, C.-L. Zou, and L. Sun, Error-transparent operations on a logical qubit protected by quantum error correction, Nat. Phys. **16**, 827 (2020).

[41] See the Supplemental Material at http://link.aps.org/supplemental/10.1103/PhysRevLett.125.110503 for proof of Lemma 1, Lemma 2, Theorem 1, Theorem 2 and examples, general construction of PI control Hamiltoninan and jump operators, exact expressions of a specific PI no-jump propagator and control Hamiltonian, demonstration of PI gates for both ancilla and central system errors and more details about the PI gates in superconducting circuits, which includes Refs. [14,15,42].

[42] P. Reinhold, S. Rosenblum, W.-L. Ma, L. Frunzio, L. Jiang, and R. J. Schoelkopf, Error-corrected gates on an encoded qubit, Nat. Phys. **16**, 822 (2020).

[43] M. B. Plenio and P. L. Knight, The quantum-jump approach to dissipative dynamics in quantum optics, Rev. Mod. Phys. **70**, 101 (1998).

[44] P. W. Shor, Scheme for reducing decoherence in quantum computer memory, Phys. Rev. A **52**, R2493 (1995).

[45] E. Knill and R. Laflamme, Theory of quantum error-correcting codes, Phys. Rev. A **55**, 900 (1997).